Enhancing Colorectal Polyps Detection using Transfer Learning on DICOM Metadata

Khadija Hicham
M2SM Laboratory, ENSAM of Rabat, Mohammed V University, Rabat, Morocco
khadija_hicham@um5.ac.ma (corresponding author)

Sara Laghmati
Department of Computer Science, Faculty of Sciences, Mohammed V University, Rabat, Morocco
saralaghmati@gmail.com

Bouchaib Cherradi
STIE Team, CRMEF Casablanca-Settat, Morocco | EEIS Laboratory, ENSET of Mohammedia, Hassan II University of Casablanca, Morocco
bouchaib.cherradi@gmail.com

Soufiane Hamida
2IACS Laboratory, ENSET of Mohammedia, Hassan II University of Casablanca, Morocco | GENIUS Laboratory, SupMTI of Rabat, Morocco
hamida@enset-media.ac.ma

Amal Tmiri
M2SM Laboratory, ENSAM of Rabat, Mohammed V University, Rabat, Morocco
b_tmiri@yahoo.fr

Received: 17 September 2024 | Revised: 5 November 2024 | Accepted: 28 November 2024

 DOI: https://doi.org/10.48084/etasr.9024

ABSTRACT

Colorectal and Rectum Cancer (CRC) presents significant global health challenges, necessitating early detection and precise diagnosis to achieve effective treatment and better patient outcomes. Transfer learning techniques have shown considerable promise, especially in cancer detection. This study presents a CRC prevention system based on a fusion of a pre-trained VGG16 model with dense layers for metadata processing. Experiments were performed using the CT Colonography dataset from The Cancer Imaging Archive (TCIA), applying preprocessing and class weighting to address class imbalance. The system was evaluated using accuracy, loss, recall, precision, F1-score, and AUC. This study investigated the impact of integrating DICOM patient metadata to enhance the proposed CRC prevention system. The findings indicate that the proposed MetaVGGNet model outperformed the standard VGG16, achieving greater accuracy (82%) and a marginally lower loss. This successful application has the potential to enhance CRC diagnosis and treatment and underscores the importance of incorporating metadata into deep learning classification systems, offering avenues for more effective and dependable diagnostic tools in CRC management.

Keywords-DICOM metadata; CRC prognosis; transfer learning; polyps detection

I. INTRODUCTION

According to the World Health Organization (WHO), in 2020, approximately 1.93 million new cases of Colorectal Cancer (CRC) were diagnosed worldwide, with projections indicating a significant increase to 3.2 million new cases by 2040, representing a 63% increase, and a 73% increase in mortality, with 1.6 million deaths per year [1]. Early detection of CRC is crucial, as it improves treatment outcomes and increases survival rates. CRC originates from precancerous growths in the intestinal lining, spurred by mutations in genes that regulate cell growth, activation of cancer-causing genes, alterations in immune responses, and possibly influenced by changes in the gut microbiome [2]. CRC polyps are critical precursors to CRC development that promote cancer progression. Although most polyps do not evolve into CRC,

their presence enables preventive interventions due to their extended transformation period of progression to CRC [3, 4]. Ignored polyps can transform into CRC [5]. Screening methods include colonoscopy and CT Colonography (CTC) [6, 7].

CTC and colonoscopy are widely used methods for detecting colorectal polyps. Colonoscopy has a sensitivity of 95-100% in detecting polyps larger than 6 mm and a specificity close to 100%, as it allows direct visualization and polyp removal during the procedure. In contrast, CT colonography has a sensitivity ranging from 85-93% for polyps greater than 10 mm and 70-86% for polyps 6-9 mm, with a lower sensitivity for smaller polyps (less than 6 mm). Its specificity ranges from 86-97%. Although colonoscopy is often considered the gold standard due to its ability to both detect and remove polyps during the procedure, research indicates that CTC is a safe and cost-effective substitute for colonoscopy in colorectal screening [8-10]. The non-invasive nature of CT colonography reduces patient discomfort and avoids the risks associated with sedation. When abnormalities are detected, a follow-up colonoscopy can be used to remove polyps, making CT colonography an excellent initial screening tool. Digital Imaging and Communications in Medicine (DICOM) is a standard format for medical imaging data, commonly used in CT scans [11, 12].

Deep Learning (DL) methods have exhibited notable advances in the classification and diagnosis of CRC, offering several advantages over traditional approaches [13]. A variety of studies have explored the classification of polyps using Convolutional Neural Networks (CNNs), showing promising results in accurately identifying different types of colorectal polyps. For instance, in [14] EfficientNet-B7 and EfficientNet-b0 were used to classify polyps with high accuracy. In [15], the VGG16 and VGG19 architectures were used to classify colon polyps on CT scans, demonstrating the potential of DL techniques in helping radiologists with early detection. In [16], a CNN achieved 94% accuracy in classifying traditional adenomas, sessile serrated adenomas, and hyperplastic polyps. These findings collectively highlight the effectiveness of CNN in the precise classification of polyps.

Transfer Learning (TL) techniques [17-18], leveraging pre-trained models such as AlexNet and VGG16 [13, 19], have further increased performance, outperforming models trained from scratch in CRC, particularly, and in medical tasks, generally. Performance comparisons across various tasks indicate the superiority of deep TL with AlexNet for CRC lymph node metastasis classification [20-22]. VGG16 TL has been successfully applied in various medical imaging tasks, such as Alzheimer's disease diagnosis [23], lung cancer detection [24], and COVID-19 detection on chest CT scans [25]. These studies demonstrate the effectiveness of utilizing pre-trained VGG16 models for accurate and efficient medical classification tasks. The TL approach with VGG16 has consistently shown high accuracies ranging from 86% to 99.54% across different medical imaging applications. Therefore, leveraging VGG16 TL for CRC prevention could potentially lead to promising outcomes by utilizing the model's pre-trained features to enhance the classification of CRC-related images, aiding in early diagnosis.

DICOM stores medical images along with descriptive metadata, such as patient information, details of the imaging technique, and more [26-29]. The use of metadata in DICOM images plays a crucial role in various aspects of medical imaging. In [30], Modality Mapping and Orchestration MOMO was proposed, which is a DL-based approach to automate the classification of external DICOM studies based on the Picture Archiving and Communication Systems (PACS) archive consisting of 11,934 imaging series with anatomical labels. This study combined metadata analysis with neural network ensembles to automate the mapping process, showcasing the potential of DL, including DenseNet-161 and ResNet-152, alongside metadata matching in classifying external DICOM studies. In [31], the DICOM standard was implemented for digital pathology, focusing on extracting pixel data, pixel-related metadata, patient data, and specimen-related metadata. This study evaluated how effectively the DICOM standard could be used in a healthcare network involving multiple sites and vendors, highlighting both the capabilities and limitations of using DICOM metadata in the context of pathology. In [32], the focus was on extracting exposure parameters and dose-relevant indexes of CT examinations from DICOM metadata using an automated Matlab-based approach. This study aimed to extract information from structured elements in DICOM metadata relevant to exposure, showcasing the importance of metadata in medical imaging.

II. METHODOLOGY

A. Proposed CRC Prevention System

The proposed CRC prevention system encompasses a series of steps aimed at optimizing the detection of colon polyps in medical images. Initially, Region of Interest (ROI) and slice selection techniques were employed, leveraging polyp emplacement data to selectively extract relevant slices for analysis. Computational efforts focused solely on pertinent data and streamlining subsequent analyses. Resizing and normalization procedures were implemented to further refine the dataset. Resizing involved reducing the width and height dimensions of the initial scans from 512 to 128 pixels. Normalization standardized pixel values across images, ensuring consistency in image intensity ranges and mitigating potential disparities arising from variations in acquisition settings or equipment. Metadata integration played a crucial role in the classification approach, where features such as patient age and sex were selected to enrich contextual insights and enhance model interpretability, as clinicians can better understand the model output in the context of a patient's demographic and clinical characteristics. Moreover, to address the class imbalance inherent in the dataset, class weights were employed, assigning higher weights to underrepresented classes to improve model sensitivity and classification accuracy. After the preprocessing steps, TL was used by employing the VGG-16 model, leveraging its pre-trained features to accelerate training and enhance polyp detection. This approach not only reduces computational requirements but also facilitates faster convergence and improved performance, laying the groundwork for a robust CRC prevention system. Figure 1 displays the flow diagram of the proposed system.

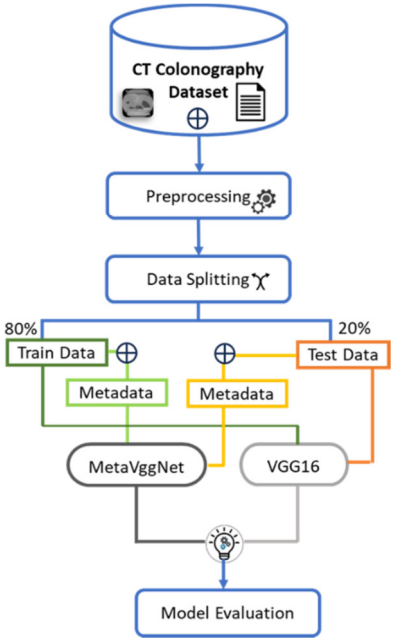

Fig. 1. Flowchart of the proposed CRC prevention system.

B. Dataset Description

This study utilized the CT Colonography dataset generously provided by the American College of Radiology Imaging Network (ACRIN), which offers access to a subset of the CTC trial data hosted on TCIA under CT Colonography (ACRIN 6664) [33]. This dataset, which consists of DICOM-formatted files, comprises a substantial collection of 825 cases, 3451 series, and 941,771 images, totaling 462.6 GB in size. The inclusion of spreadsheets further facilitates the identification of positive and negative polyp cases within the dataset. CT scans, renowned for their ability to produce three-dimensional representations of scanned objects, yield a series of 2D image slices, each encapsulated within a DICOM file enriched with vital metadata. These metadata include comprehensive patient information, crucial imaging parameters, and precise spatial orientation details.

C. Preprocessing

The polyp emplacement information provided in the xls sheet was utilized to selectively extract only the slices containing polyps, minimizing the required computational resources. Images lacking polyp placement information were excluded from the selection process. Additionally, for images classified as polyp-free by professionals, the central slice was extracted. This approach ensured that computational efforts focused solely on relevant data, optimizing efficiency and streamlining subsequent analyses. Additionally, the width and height of the initial scans were resized from 512 to 128 pixels. This resizing operation reduced the computational burden associated with handling large-scale data and also optimized the data representation for subsequent analysis. Scaling down the dimensions condensed the information while preserving essential features.

D. Class Weights

Class weights were employed to address the inherent class imbalance in the dataset. The number of instances belonging to the class without polyps significantly outweighed those of images with polyps, potentially leading to biased model performance. Higher weights were assigned to the underrepresented classes (polyp-positive scans) during model training. Assigning appropriate weights ensured that the model's learning process was more sensitive to minority classes, improving its ability to accurately classify both polyp and polyp-free scans. Weights were assigned to each class based on the following equation:

$$WeightClass_i = \frac{TS}{2Ns_i} \quad (1)$$

where $i \in$ {Polyp_free, polyp}, TS denotes the total number of samples of the dataset, and NS represents the number of samples in class i.

E. Transfer Learning with VGG16

The VGG-16 model is a widely recognized CNN architecture pre-trained on ImageNet that offers a robust framework to capitalize on the learned features from a diverse range of images, accelerate the training process, and enhance the accuracy of polyp detection. This approach not only reduces the need for extensive computational resources and labeled data but also facilitates faster convergence and improved performance on this specific medical imaging task. Figure 2 illustrates the architecture of the proposed model, named MetaVggNet. It comprises two inputs: an image input and a textual input. These inputs are fed into a feature extraction block that incorporates the VGG16 model alongside dense and dropout layers. The final output layer consists of a single neuron that utilizes the sigmoid activation function. This study utilized the VGG16 architecture as a base model, leveraging its pre-trained weights from ImageNet while excluding its top layers. All layers are frozen to retain these pre-trained weights. The image features are extracted from the VGG16 model and flattened, while the metadata is processed through dense layers. The resulting features are concatenated, and a dropout layer is incorporated to mitigate overfitting.

F. Evaluation Metrics

The performance of the model was evaluated by generating a Confusion Matrix (CM), effectively summarizing the model's performance by comparing the predicted with actual labels [34]. The CM includes counts for various classifications: True Positives (TP), indicating correctly identified abnormal scans, False Positives (FP), representing normal scans incorrectly classified as abnormal, True Negatives (TN), where normal scans are correctly identified, and False Negatives (FN), denoting abnormal scans incorrectly classified as normal. Various metrics were used to evaluate the model, including Accuracy (Acc), Precision (Pre), Recall (Rec), and F1-score (F1). The following equations define the metrics used:

$$\text{Accuracy} = \frac{\text{TP+TN}}{\text{TP+FP+TN+FN}} \quad (2)$$

$$\text{Precision} = \frac{\text{TP}}{\text{TP+FP}} \quad (2)$$

$$\text{Recall} = \text{TP}/(\text{TP} + \text{FN}) \quad (3)$$

$$\text{F1} = \frac{2\text{TP}}{2\text{TP}+\text{FN}+\text{FP}} \quad (4)$$

The Receiver Operating Characteristic (ROC) is a crucial tool in DL. ROC curves illustrate a model's ability to correctly identify positive cases while minimizing the misclassification of negative cases. The horizontal axis of the ROC curve depicts the FP rate, while the vertical axis represents the TP rate. A model is considered more effective if its ROC curve is placed closer to the y-axis [35].

III. RESULTS AND DISCUSSION

This study investigated the impact of metadata on the performance of the CTC prevention system by comparing VGG16 with MetaVGGNet. TensorFlow 1.5.2 was used, with an Intel Xeon CPU and 14 GB of RAM. The dataset was divided into training/testing with an 80:20 ratio. The validation set used 20% of the training set.

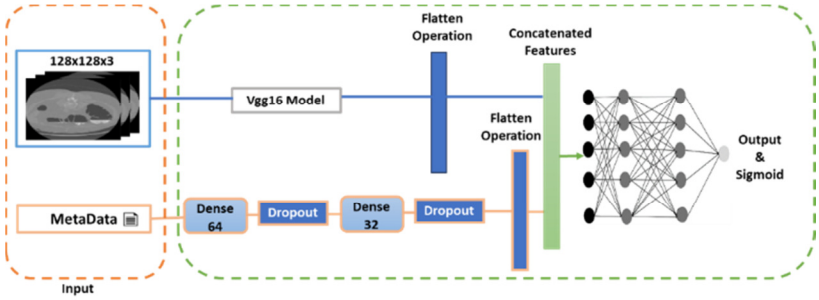

Fig. 2. The proposed MetaVggNet model.

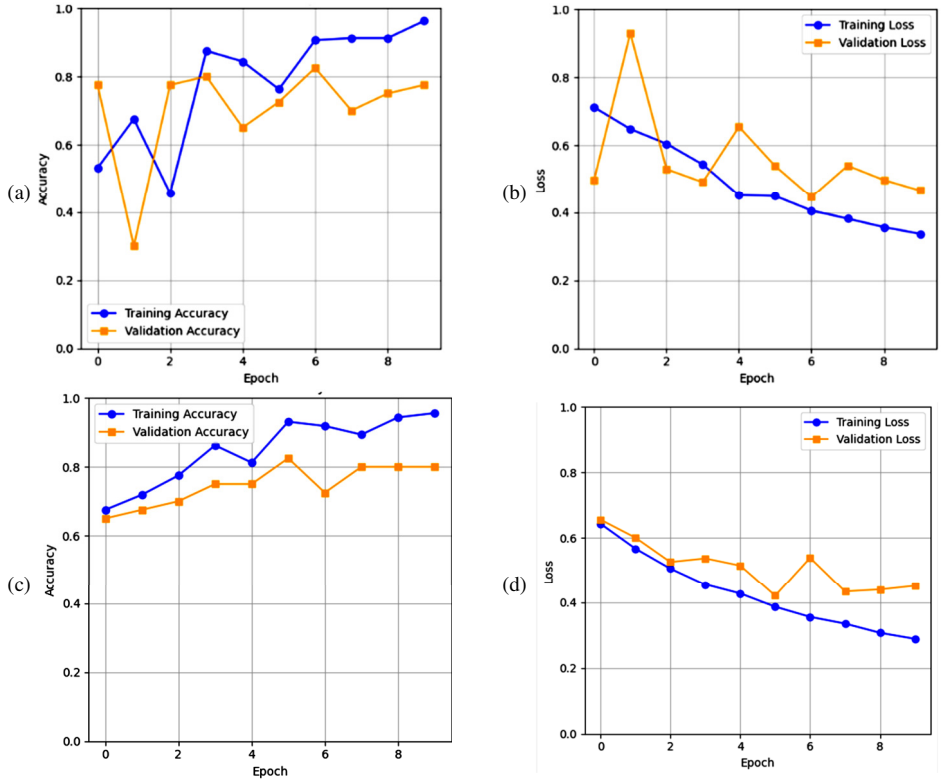

Fig. 3. Training and validation performance curves: (a) Vgg16 accuracy, (b) VGG16 loss, (c) MetaVGGNet accuracy, (d) MetaVGGNet loss.

A. *Training and Validation Results*

During model training, the number of epochs was set to 10, determining the number of times that the entire dataset would pass through the model. The batch size, set to 32, determines the number of samples propagated through the network at each step. The class weight parameter was used to adjust the contribution of different classes to the loss function during training, which is especially useful for imbalanced datasets. The validation split parameter was set to 0.2, indicating that 20% of the training data was reserved for validation, allowing to monitor the model performance on unseen data after each

epoch, helping to prevent overfitting and improve generalization. The Adam optimizer was used with the loss function set to binary_crossentropy, which is suitable for binary classification problems, making the model capable of efficiently updating the weights to minimize the loss during training.

Table I presents the performance comparison between VGG16 and VGG16 with metadata (MetaVGGNet). The standard VGG16 model achieved an accuracy of 91.2% on the training set with a loss of 0.36, and 75% accuracy on the validation set with a loss of 0.49. Performance improved significantly with the addition of metadata. The VGG16 model with metadata achieved an impressive accuracy of 95.6% on the training set with a loss of 0.29 and 80% accuracy on the validation set with a loss of 0.45. This improvement indicates the importance and effectiveness of incorporating metadata, which resulted in a notable enhancement in the model's ability to generalize.

TABLE I. VGG16 ACCURACY AND LOSS FOR TRAINING AND VALIDATION WITH AND WITHOUT METADATA

Models	Training		Validation	
	Acc	Loss	Acc	Loss
VGG16	91.2%	0.36	75%	0.49
MetaVGGNet	95.6%	0.29	80%	0.45

B. Testing Results

Figure 6 shows the CM for the testing phase, including 50 samples, which was used to calculate accuracy, loss, precision, recall, F1-score, and the ROC curve to further evaluate the models' performance on the CT colonography dataset.

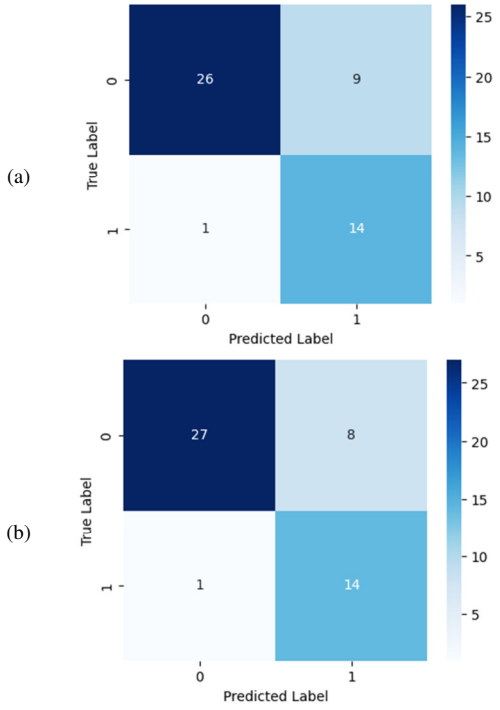

Fig. 4. CMs for (a) VGG16, (b) MetaVGGNet.

As shown in these CMs, the inclusion of metadata in the VGG16 model resulted in a reduction in FP, enhancing the model's ability to accurately classify instances. This improvement is indicated by the decrease in FP from 9 to 8, while other metrics remain constant.

Table II shows the results in terms of precision, recall, and F1-score on the test data. The VGG16 model with metadata demonstrated an improvement in the identification of both cases. For polyp_free cases, the addition of metadata resulted in a 3% increase in recall and an improved F1-score (0.86). Similarly, for cases with a polyp, the MetaVGGNet model achieved a 3% increase in accuracy and a notable improvement in the F1-score, reaching 0.76. These results emphasize the importance of metadata in enhancing the model's performance and its ability to identify polyps.

TABLE II. TESTING RESULTS FOR EACH MODEL

Models	Classes	Prec	Rec	FS
VGG16	Polyp free	96%	74%	0.84
	with polyp	61%	93%	0.74
MetaVGGNet	Polyp free	96%	77%	0.86
	With polyp	64%	93%	0.76

The VGG16 model with metadata shows an improvement in test accuracy compared to the standard VGG16 model. While the VGG16 model achieved an accuracy of 80%, the MetaVGGNet model achieved an accuracy of 82%, showcasing the effectiveness of incorporating metadata to enhance the model's performance. Additionally, the test loss decreased from 0.46 for the VGG16 model to 0.45 for the VGG16 model with metadata, further emphasizing the advantages of including metadata.

Figure 7 shows a ROC curve comparison between the VGG16 model and the VGG16 model with metadata, indicating a slightly higher AUC for the latter. This indicates that the VGG16 model with metadata has a slightly better ability to distinguish between positive and negative cases compared to the standard VGG16.

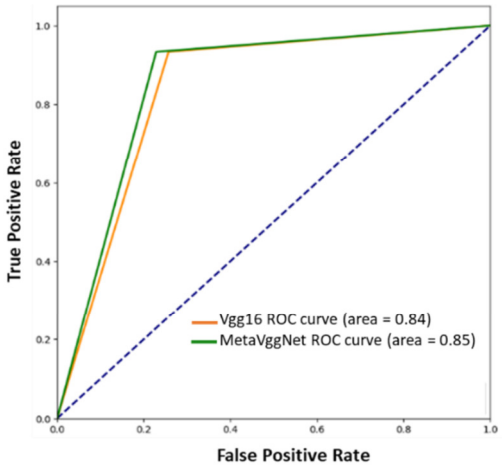

Fig. 5. ROC curves of the models.

C. Comparative Study

Making a direct comparison between different studies can be challenging due to the use of different datasets and architectures. VGG16 was used to detect Alzheimer's in [23] and for COVID-19 in [25]. In [36], 3DCNN is used for the prediction of tuberculosis on CT scans. These studies showed accuracies ranging from 67.5% to 99.54% across different diseases. The results of this study fall in this range, with an accuracy of 82%, recall of 93% for cases with polyps, and an AUC of 0.85, although the dataset is limited. In general, including metadata can be a promising approach to enhance model performance.

IV. CONCLUSION

This study introduced MetaVggNet, a model based on VGG16, designed to take advantage of both images and associated metadata to improve the task of CT scan classification on the absence or presence of polyps. Experiments were carried out using the CT Colonography dataset, subjecting it to preprocessing from selection through resizing until normalization. Class weighting was used to address class imbalance. TL was exploited, integrating additional layers to process metadata along with image features. The results showed that the MetaVggNet model outperformed the standard VGG16 model in all metrics evaluated. Including metadata enhanced the model performance in terms of accuracy, precision, recall, and the area under the ROC curve. In particular, the model with metadata demonstrated a reduction in false positives, indicating improved classification accuracy. Therefore, incorporating metadata into a TL model improves its performance. These findings underscore the importance of including metadata to enhance the performance of DL models in medical imaging tasks.

Despite the improved performance of MetaVggNet, certain limitations are present. As the CT Colonography dataset used for training was relatively limited in size, larger and more diverse datasets could further validate the model's generalizability. The performance of MetaVggNet is highly dependent on the quality of the metadata. In clinical practice, metadata can sometimes be incomplete or inconsistently recorded, which could impact the model's real-world performance. The additional layers for metadata processing increase the model's complexity, requiring more computational resources and training time compared to standard VGG16. To further improve MetaVggNet and extend its applicability, the integration of additional modalities with image and metadata information can be explored. Future research could also focus on fine-tuning the model. Also, incorporating Explainable AI (XAI) would help clinicians understand the model's decision-making process.

REFERENCES

[1] Y. Xi and P. Xu, "Global colorectal cancer burden in 2020 and projections to 2040," *Translational Oncology*, vol. 14, no. 10, Oct. 2021, Art. no. 101174, https://doi.org/10.1016/j.tranon.2021.101174.

[2] B. C. Y. Tse, Z. Welham, A. F. Engel, and M. P. Molloy, "Genomic, Microbial and Immunological Microenvironment of Colorectal Polyps," *Cancers*, vol. 13, no. 14, Jan. 2021, Art. no. 3382, https://doi.org/10.3390/cancers13143382.

[3] M. Øines, L. M. Helsingen, M. Bretthauer, and L. Emilsson, "Epidemiology and risk factors of colorectal polyps," *Best Practice & Research Clinical Gastroenterology*, vol. 31, no. 4, pp. 419–424, Aug. 2017, https://doi.org/10.1016/j.bpg.2017.06.004.

[4] K. Hicham, S. Laghmati, and A. Tmiri, "3D CT Scans for Colorectal Cancer Classification using VGG16 and Data Augmentation," in *2023 10th International Conference on Wireless Networks and Mobile Communications (WINCOM)*, Istanbul, Turkiye, Oct. 2023, pp. 1–4, https://doi.org/10.1109/WINCOM59760.2023.10322904.

[5] J. E. G. IJspeert, B. A. J. Bastiaansen, and E. Dekker, "Serrated polyposis syndrome: a silent killer when undetected," *Endoscopy*, vol. 48, no. S 1, Dec. 2016, https://doi.org/10.1055/s-0042-101385.

[6] J. J. Näppi *et al.*, "Automated detection of colorectal polyps in photon-counting CT colonography," in *Medical Imaging 2023: Imaging Informatics for Healthcare, Research, and Applications*, Apr. 2023, vol. 12469, pp. 187–191, https://doi.org/10.1117/12.2654292.

[7] C. M. Sakai *et al.*, "A Head-to-Head Comparison of Computed Tomography Colonography, Optical Colonoscopy, and Colon Endoscopic Capsule for the Detection of Polyps After Partial Colectomy or Rectosigmoidectomy for Colorectal Cancer: A Pilot Study," *Cureus*, vol. 15, no. 5, Art. no. e38410, https://doi.org/10.7759/cureus.38410.

[8] W. Bai *et al.*, "Diagnostic accuracy of computed tomography colonography in patients at high risk for colorectal cancer: a meta-analysis," *Colorectal Disease*, vol. 22, no. 11, pp. 1528–1537, 2020, https://doi.org/10.1111/codi.15060.

[9] O. Svystun, M. Zeman, M. Seidler, and C. Fung, "CT Colonography Versus Optical Colonoscopy: Cost-Effectiveness in Colorectal Cancer Screening," *EMJ Innovations*, Oct. 2022, https://doi.org/10.33590/emjinnov/10035977.

[10] O. Svystun, M. Zeman, M. Seidler, and C. Fung, "92 CT colonography vs optical colonoscopy: an Alberta-based cost effectiveness analysis for colorectal cancer screening," *BMJ Evidence-Based Medicine*, vol. 27, no. Suppl 1, Jun. 2022, https://doi.org/10.1136/bmjebm-2022-PODabstracts.37.

[11] M. Rutherford *et al.*, "A DICOM dataset for evaluation of medical image de-identification," *Scientific Data*, vol. 8, no. 1, Jul. 2021, Art. no. 183, https://doi.org/10.1038/s41597-021-00967-y.

[12] K. Hicham, S. Laghmati, and A. Tmiri, "Artificial Intelligence for Colorectal Polyps Classification Using 3D CNN," in *Advances in Integrated Design and Production II*, Rabat, Morocco, 2023, pp. 165–174, https://doi.org/10.1007/978-3-031-23615-0_17.

[13] R. D. Dondapati, T. Sivaprakasam, and K. V. Kumar, "Dermatological Decision Support Systems using CNN for Binary Classification," *Engineering, Technology & Applied Science Research*, vol. 14, no. 3, pp. 14240–14247, Jun. 2024, https://doi.org/10.48084/etasr.7173.

[14] V. Panteris *et al.*, "A Deep Learning Model for Classifying Histological Types of Colorectal Polyps," in *Studies in Health Technology and Informatics*, J. Mantas, P. Gallos, E. Zoulias, A. Hasman, M. S. Househ, M. Charalampidou, and A. Magdalinou, Eds. IOS Press, 2023.

[15] K. Hicham, S. Laghmati, S. Hamida, A. E. Ghazi, A. Tmiri, and B. Cherradi, "Assessing the Performance of Deep Learning Models for Colon Polyp Classification using Computed Tomography Scans," in *2023 3rd International Conference on Innovative Research in Applied Science, Engineering and Technology (IRASET)*, Mohammedia, Morocco, May 2023, https://doi.org/10.1109/IRASET57153.2023.10152889.

[16] M. H. Shen *et al.*, "Deep Learning Empowers Endoscopic Detection and Polyps Classification: A Multiple-Hospital Study," *Diagnostics*, vol. 13, no. 8, Jan. 2023, Art. no. 1473, https://doi.org/10.3390/diagnostics13081473.

[17] N. Narayan Das, N. Kumar, M. Kaur, V. Kumar, and D. Singh, "Automated Deep Transfer Learning-Based Approach for Detection of COVID-19 Infection in Chest X-rays," *IRBM*, vol. 43, no. 2, pp. 114–119, Apr. 2022, https://doi.org/10.1016/j.irbm.2020.07.001.

[18] N. Kumar, M. Gupta, D. Gupta, and S. Tiwari, "Novel deep transfer learning model for COVID-19 patient detection using X-ray chest images," *Journal of Ambient Intelligence and Humanized Computing*, vol. 14, no. 1, pp. 469–478, Jan. 2023, https://doi.org/10.1007/s12652-021-03306-6.

[19] N. Kumar, A. Hashmi, M. Gupta, and A. Kundu, "Automatic Diagnosis of Covid-19 Related Pneumonia from CXR and CT-Scan Images," *Engineering, Technology & Applied Science Research*, vol. 12, no. 1, pp. 7993–7997, Feb. 2022, https://doi.org/10.48084/etasr.4613.

[20] Z. Cao *et al.*, "A Deep Learning Approach for Detecting Colorectal Cancer via Raman Spectra," *BME Frontiers*, vol. 2022, Jan. 2022, Art. no. 9872028, https://doi.org/10.34133/2022/9872028.

[21] J. Li, P. Wang, Y. Zhou, H. Liang, and K. Luan, "Different Machine Learning and Deep Learning Methods for the Classification of Colorectal Cancer Lymph Node Metastasis Images," *Frontiers in Bioengineering and Biotechnology*, vol. 8, Jan. 2021, https://doi.org/10.3389/fbioe.2020.620257.

[22] C. Srinivas *et al.*, "Deep Transfer Learning Approaches in Performance Analysis of Brain Tumor Classification Using MRI Images," *Journal of Healthcare Engineering*, vol. 2022, no. 1, 2022, Art. no. 3264367, https://doi.org/10.1155/2022/3264367.

[23] H. H. Luong, P. T. Vo, H. C. Phan, N. L. D. Tran, H. Q. Le, and H. T. Nguyen, "Fine-Tuning VGG16 for Alzheimer's Disease Diagnosis," in *Complex, Intelligent and Software Intensive Systems*, 2023, pp. 68–79, https://doi.org/10.1007/978-3-031-35734-3_8.

[24] K. Ramanjaneyulu, K. H. Kumar, K. Snehith, G. Jyothirmai, and K. V. Krishna, "Detection and Classification of Lung Cancer Using VGG-16," in *2022 International Conference on Electronic Systems and Intelligent Computing (ICESIC)*, Chennai, India, Apr. 2022, pp. 69–72, https://doi.org/10.1109/ICESIC53714.2022.9783556.

[25] M. Gomroki, R. Shah-Hosseini, and M. Hasanlou, "Rapid Automatic Detection of Covid-19 in Chest CT-Images Using VGG-16 and Transfer Learning," *The International Archives of the Photogrammetry, Remote Sensing and Spatial Information Sciences*, vol. XLVIII-4/W2-2022, pp. 39–44, Jan. 2023, https://doi.org/10.5194/isprs-archives-XLVIII-4-W2-2022-39-2023.

[26] W. Gohn, H. Govindaraju, P. Faley, F. Massanes-Basi, and A. H. Vija, "DICOM data storage and retrieval with MongoDB," in *Medical Imaging 2022: Imaging Informatics for Healthcare, Research, and Applications*, Apr. 2022, vol. 12037, pp. 129–133, https://doi.org/10.1117/12.2613287.

[27] M. Napravnik *et al.*, "Using Autoencoders to Reduce Dimensionality of DICOM Metadata," in *2022 International Conference on Electrical, Computer, Communications and Mechatronics Engineering (ICECCME)*, Maldives, Nov. 2022, pp. 1–6, https://doi.org/10.1109/ICECCME55909.2022.9988310.

[28] Z. Long, A. I. Walz-Flannigan, L. A. Littrell, and B. A. Schueler, "Technical note: Four-year experience with utilization of DICOM metadata analytics in clinical digital radiography practice," *Medical Physics*, vol. 50, no. 2, pp. 831–836, 2023, https://doi.org/10.1002/mp.16170.

[29] H. J. Hazarika, S. Ravikumar, and A. Handique, "Developed DICOM standard schema with DSpace," *Collection and Curation*, vol. 41, no. 2, pp. 50–61, Aug. 2021, https://doi.org/10.1108/CC-05-2021-0015.

[30] F. Jonske *et al.*, "Deep Learning–driven classification of external DICOM studies for PACS archiving," *European Radiology*, vol. 32, no. 12, pp. 8769–8776, Dec. 2022, https://doi.org/10.1007/s00330-022-08926-w.

[31] M. D. Herrmann *et al.*, "Implementing the DICOM Standard for Digital Pathology," *Journal of Pathology Informatics*, vol. 9, no. 1, Jan. 2018, Art. no. 37, https://doi.org/10.4103/jpi.jpi_42_18.

[32] J. K. Dave and E. L. Gingold, "Extraction of CT Dose Information From DICOM Metadata: Automated Matlab-Based Approach," *American Journal of Roentgenology*, vol. 200, no. 1, pp. 142–145, Jan. 2013, https://doi.org/10.2214/AJR.12.8501.

[33] K. Clark *et al.*, "The Cancer Imaging Archive (TCIA): Maintaining and Operating a Public Information Repository," *Journal of Digital Imaging*, vol. 26, no. 6, pp. 1045–1057, Dec. 2013, https://doi.org/10.1007/s10278-013-9622-7.

[34] R. M. Mathew and R. Gunasundari, "A Cluster-based Undersampling Technique for Multiclass Skewed Datasets," *Engineering, Technology & Applied Science Research*, vol. 13, no. 3, pp. 10785–10790, Jun. 2023, https://doi.org/10.48084/etasr.5844.

[35] S. Laghmati, S. Hamida, K. Hicham, B. Cherradi, and A. Tmiri, "An improved breast cancer disease prediction system using ML and PCA," *Multimedia Tools and Applications*, vol. 83, no. 11, pp. 33785–33821, Mar. 2024, https://doi.org/10.1007/s11042-023-16874-w.

[36] H. Zunair, A. Rahman, N. Mohammed, and J. P. Cohen, "Uniformizing Techniques to Process CT Scans with 3D CNNs for Tuberculosis Prediction," in *Predictive Intelligence in Medicine*, Lima, Peru, 2020, pp. 156–168, https://doi.org/10.1007/978-3-030-59354-4_15.